Biol. Cybern. 81, 3–9 (1999)

Biological Cybernetics

An autoregressive method for the measurement of synchronization of interictal and ictal EEG signals

Piotr J. Franaszczuk[1,2], **Gregory K. Bergey**[1,2,3]

[1] Department of Neurology, University of Maryland School of Medicine, Baltimore, MD 21201, USA
[2] Maryland Epilepsy Center, University of Maryland Medical Center, Baltimore, Maryland, USA
[3] Department of Physiology, University of Maryland School of Medicine, Baltimore, Maryland, USA

Received: 20 July 1997 / Accepted in revised form: 26 January 1999

Abstract. We propose a new measure of synchronization of multichannel ictal and interictal EEG signals. The measure is based on the residual covariance matrix of a multichannel autoregressive model. A major advantage of this measure is its ability to be interpreted both in the framework of stochastic and deterministic models. A preliminary analysis of EEG data from three patients using this measure documents the expected increased synchronization during ictal periods but also reveals that increased synchrony persists for prolonged periods (up to 2 h or more) in the postictal period.

1 Introduction

Epileptic seizures are by nature episodic events. Experimental models of epilepsy, as well as patient observations, suggest that the transition to ictal events is characterized by an abnormal increase in synchronization of neural activity. Although neuronal synchronization is the hallmark of an ictal event, changes in network synchrony may precede or follow the actual ictal event.

The electrical activity of the brain recorded as EEG signals has been analyzed either as random stochastic processes or as realizations of nonlinear dynamic processes exhibiting chaotic behavior. During the last decade, numerous researchers have reported evidence of low-dimensional chaos in the human electroencephalogram based on estimating Lyapunov exponents or geometric invariants of the underlying attractor, such as the correlation dimension (see review by Pritchard and Duke 1992). Recently, however, after more careful examination of data with improved algorithms, some authors have found no evidence of low-dimensional chaos in the normal human EEG (Pritchard et al. 1995; Palus 1996; Theiler and Rapp 1996). Indeed, the only instance where nonlinear dynamic approaches have proved to be beneficial was in analyses of signals recorded from electrodes in close proximity to the epileptic focus (Pijn et al. 1991, 1997; Casdagli et al. 1996; Elger and Lehnertz 1998) shortly before and during seizures.

Most of the reports of nonlinear applications have been based on single channel analyses and results from different channels were then subsequently compared. Iasemidis and Sackellares (1996) suggested that the onset of a seizure represents a spatiotemporal transition from a complex to a less complex (more ordered) state. They also suggested that this transition occurs only if conditions of a long-term spatiotemporal dynamical entrainment of a critical mass of interconnected regions of brain are met. Lehnertz and Elger (1995, 1997) demonstrated decreased neuronal complexity in the primary epileptogenic area in preictal, ictal and postictal states. Interpretation of these results has to be done with caution, however, since estimates of nonlinear measures from short nonstationary time series may result in incorrect estimates and ambiguous interpretations.

Another approach to EEG analysis has been motivated by the assumption that the EEG is generated by a stochastic system. Nonparametric spectral methods utilizing fast Fourier transform (FFT) and parametric methods based on autoregressive models (AR) have been shown to be useful in analyzing normal and ictal EEG (Franaszczuk et al. 1985; Gath et al. 1992; Franaszczuk et al. 1994; Franaszczuk and Bergey 1998). Multichannel versions of these methods allow for measurements of synchrony between different spatial locations in brain using ordinary, partial (Franaszczuk et al. 1985; Ducrow and Spencer 1992; Gotman and Levtova 1996) or directed coherence (Wang and Takigawa 1992) and the directed transfer function (DTF) (Franaszczuk et al. 1994; Kamiński et al. 1997; Korzeniewska et al. 1997). Measurements of these functions in preictal and ictal states show increased synchrony between channels close to the epileptogenic focus. These results are in agreement with results of nonlinear analyses cited above.

Most of the previous studies employing both stochastic and deterministic approaches were applied either to compare the linear and nonlinear prediction methods (Blinowska and Malinowski 1991; Theiler et al. 1992; Scott and Schiff 1995) or to discriminate between sto-

Correspondence to: P. Franaszczuk
(e-mail: pfranasz@umaryland.edu)

chastic and deterministic models (Theiler 1995; Pijn et al. 1997). The results of such studies are often not conclusive and prone to misinterpretation. Lehnertz and Elger (1995) pointed out that "considering the huge number of influencing factors, it remains difficult to prove an EEG epoch under consideration as the product of a dynamical system that exhibits chaotic behavior rather than as colored noise." In practice, only deterministic systems of low complexity can be identified from short stationary epochs of EEG data. Recently Micheloyannis et al. (1998) demonstrated that both coherence analysis and nonlinear analyses of EEG give useful information about spatial synchronization and coupling between regions.

We propose here a multichannel autoregressive method of analysis of spatiotemporal synchronization that can be interpreted in both a stochastic and a deterministic framework, thus avoiding misinterpretation. The local and global linear autoregressive approximation has been used previously as a tool for discriminating randomness from low-dimensional chaos (Cuomo et al. 1994; Casdagli and Weigend 1993). In this study, we use the multichannel or vector autoregressive model as a tool for measuring the relative level of synchronization between channels, not attempting to distinguish between stochastic or deterministic models.

We present a preliminary application of these method to long continuous recordings of interictal, preictal, ictal and postictal recordings from subdural and depth electrodes implanted in three patients with intractable epilepsy undergoing continuous video-EEG monitoring.

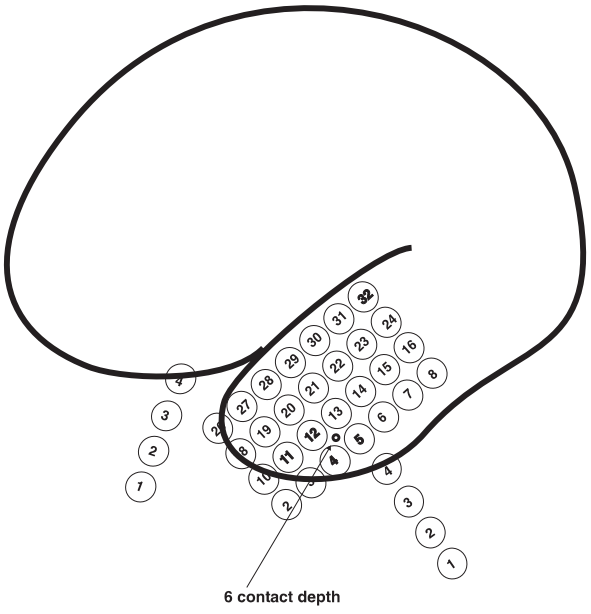

Fig. 1. Schematic diagram of subdural grids and strips used to record seizures in patient 1. The two four-contact strips were under the orbitofrontal and basal temporal regions. The six contact depth electrode was placed free hand perpendicular to the grids so that the deepest contacts were in the mesial temporal structures. Four contacts of the subdural grid (1,9,17,25) were removed to facilitate placement of the grid; the numbering of the remaining contacts was not altered

2 Data collection

Data were analyzed from seizures from three patients monitored prior to anterior temporal lobectomy for intractable complex partial seizures. All patients had intracranial EEG (ICEEG) recordings from electrode arrays combining a 28- to 32-contact subdural grid over the lateral temporal neocortex and one or two multicontact depth electrodes placed freehand through the grid so that the deepest contacts recorded from the mesial temporal structures (as confirmed by postoperative MRI; Barry et al. 1992). At times, additional subdural strips were placed over the orbitofrontal, lateral frontal or basal temporal neocortex. Decisions to perform intracranial monitoring were based on needs for functional mapping of eloquent cortex (e.g. language mapping of the dominant temporal lobe) and seizure localization. One typical schematic diagram of placement of electrodes is shown in Fig. 1. Typically, the lateral temporal grid was a 32-contact array. In some instances (e.g. Fig. 1) up to four contacts were removed to facilitate grid placement; contact numbering was not changed.

Data for seizure analysis were collected using a 64-channel video EEG recording system, the Telefactor MODAC 64-BBS, with a bandpass filter of 0.5–70 Hz. The multichannel EEG signals were digitized at a rate of 200 samples/s and stored with the corresponding video patient image on VHS video tape. Data were transferred to a Telefactor Beekeeper Digital EEG Review Workstation, then analyzed on a SGI Indigo2 workstation. All contacts were referenced to a common subdural contact on a frontal lobe grid or strip or to a contact on the edge of the temporal grid remote from the source. Seizures selected for analysis were those occurring at least 6 h after the previous seizure. Only complex partial seizures that did not secondarily generalize were selected for analysis. Epochs were selected where the states (e.g. awake, asleep) were similar before and after the seizure. Visual analysis of the EEG was performed so that seizures selected did not have prolonged postictal slowing.

Signals from all channels were normalized to zero mean and a unitary standard deviation to eliminate differences in gain from different electrodes.

3 Analysis method

The pth-order vector autoregressive process (Priestley 1981) can be expressed as:

$$\mathbf{x}_t = \sum_{j=1}^{p} \mathbf{A}_j \mathbf{x}_{t-j} + \mathbf{e}_t \quad , \tag{1}$$

where $\mathbf{A}_j$ are $m \times m$ matrices of model coefficients, $\mathbf{x}_t$ is the vector of the multichannel signal, and m is the number of channels. In the stochastic linear interpretation of this model, $\mathbf{e}_t$ is the vector of multivariate zero mean uncorrelated white noise.

Equation (1) can be converted to a state space representation by introducing an *mp*-dimensional state vector:

$$\mathbf{y}_t = (\mathbf{x}_{t-1}, \mathbf{x}_{t-2}, \ldots, \mathbf{x}_{t-p})^T \quad . \tag{2}$$

The evolution of this state vector is governed by the state transition equation:

$$\mathbf{y}_{t+1} = \mathbf{F}\mathbf{y}_t + \mathbf{z}_t \quad , \tag{3}$$

where $\mathbf{z}_t = (\mathbf{e}_t, 0, \ldots, 0)^T$ and the state transition matrix $\mathbf{F}$ is in a block-canonical form with $m \times m$ identity matrices $\mathbf{I}$ along the underdiagonal and the parameter matrices $\mathbf{A}_j$ on the top:

$$\mathbf{F} = \begin{pmatrix} \mathbf{A}_1 & \ldots & \mathbf{A}_{p-1} & \mathbf{A}_p \\ \mathbf{I} & \ldots & 0 & 0 \\ \vdots & \ddots & \vdots & \vdots \\ 0 & \ldots & \mathbf{I} & 0 \end{pmatrix} \quad . \tag{4}$$

Equation (3) is a first-order difference equation describing a Markov process in *mp*-dimensional space. This type of conversion to a state space is referred to as embedding in the dynamical-system literature.

The evolution of a dynamic system is governed by the deterministic state transition equation:

$$\frac{d\mathbf{x}(t)}{dt} = \mathbf{G}[\mathbf{x}(t)] \quad , \tag{5}$$

where the function $\mathbf{G}$ can be highly non-linear. It can be shown (e.g. Serio 1992) that periodic systems (limit cycles) and quasi-periodic systems (tori) can be thought of as autoregressive processes in the limiting case of driving white noise variance equal to zero. The number of degrees of freedom in this case is equal to two×number of frequencies. Thus, the state vector of system evolves on the attractor according to Eq. (3) with random part $\mathbf{z}_t$ equal to zero.

In case the attractor is not regular (e.g. chaotic) and function $\mathbf{G}$ in Eq. (5) is nonlinear, one can locally linearize the system by developing $\mathbf{G}$ in a Taylor series and retaining only the first-order terms (Cuomo et al. 1994). Again, in discrete time, the system will evolve approximately according to the state transition Eq. (3) with the random part $\mathbf{z}_t$ equal to zero.

In practice, even in the case of regular attractors or linear dynamical systems, one can expect measurement errors; these can be interpreted as additive stochastic noise. According to Cheng and Tong (1992), the system (5) is called a skeleton and the observed time series is a realization of a stochastic process that results from perturbing the skeleton with additive stochastic noise. This notion allows one to use standard methods of fitting autoregressive models to time series regardless of the underlying deterministic or stochastic model. For these studies, we used a multichannel Levinson algorithm (Marple 1987) to solve Yule-Walker equations. In this sense, the residual covariance $m \times m$ matrix $\mathbf{V}_e$ of noise vector $\mathbf{e}_t$ reflects the goodness of fit of a linear model to data.

One can expect that if the embedding dimension (equal to *mp*) is larger than the number of degrees of freedom of the system, the fit should be good (i.e. the residuals will tend to zero). If the complexity of the system is large or the system is stochastic, the residuals will be larger. As a goodness of fit measure we are using $s = \log[\det(\mathbf{V}_e)]$. For a purely uncorrelated multivariable Gaussian normalized white noise, $\mathbf{V}_e$ is a diagonal identity matrix and $s = 0$, setting the upper bound value for s. For a purely deterministic linear system or a dynamical system on a periodic or quasi-periodic trajectory, the matrix $\mathbf{V}_e$ represents a covariance matrix of measurement errors (see above), setting the lower bound value for s. For chaotic or stochastic colored-noise systems the value of s will be between these bounds.

To compare values of s in different time intervals, one has to choose the same model order p for all data epochs. This may not result in an optimal fit for some epochs. For these studies, the optimal order (according to the multichannel Akaike AIC criterion) was computed for all epochs. For EEG data with a sufficiently large (>6) number of channels, the optimal model order varies only between two or three values (e.g. 3, 4 or 5) for much of both ictal and interictal epochs with only occasional other values (Fig. 2). A uniform preset model order was chosen for all epochs so that this value was within 1 of the optimal order. If the minimum AIC was not within ±1 of the preset value, the model was not fitted and s was assigned a value of zero. $S = 0$ was used to represent missing data in the resulting plot because this is a value that cannot be generated from actual data (unless the data were pure white noise). Kitagawa and Gersh (1996) pointed out that even if fitting the autoregressive model to data is only an approximation to the unknown infinite-dimensional model, the AIC provides the asymptotically efficient solution to select the best fit to the data. The other parameter of the procedure is the length N of the epoch to use for fitting the AR model. The epochs should appear to be quasi-stationary but be long enough to allow for fitting multiparameter models. Our experience with both ictal and spontaneous EEG data (Franaszczuk et al. 1985, 1994; Franaszczuk and Bergey 1998) suggests 1000 points per channel (5 s) epochs as optimal for much of the data.

Computations were performed on continuous (1.5–6 h) recordings from groups of 7–45 channels, including seizures and periods preceding and following the seizures. The criteria for selection of seizure for analyses are described in Sect. 2.

4 Application to EEG data

Analysis of data recorded for seizures from three patients revealed the most prominent changes in the $s = \log[\det(\mathbf{V}_e)]$ for the quasi-stationary epochs during the ictal period. These changes to lower values of s reflect a better fit to a linear model, i.e. higher spatiotemporal synchronization. This results from increased correlation between channels and a more regular pattern of the signal. The lower values of s were observed not only during the seizure but also persisted

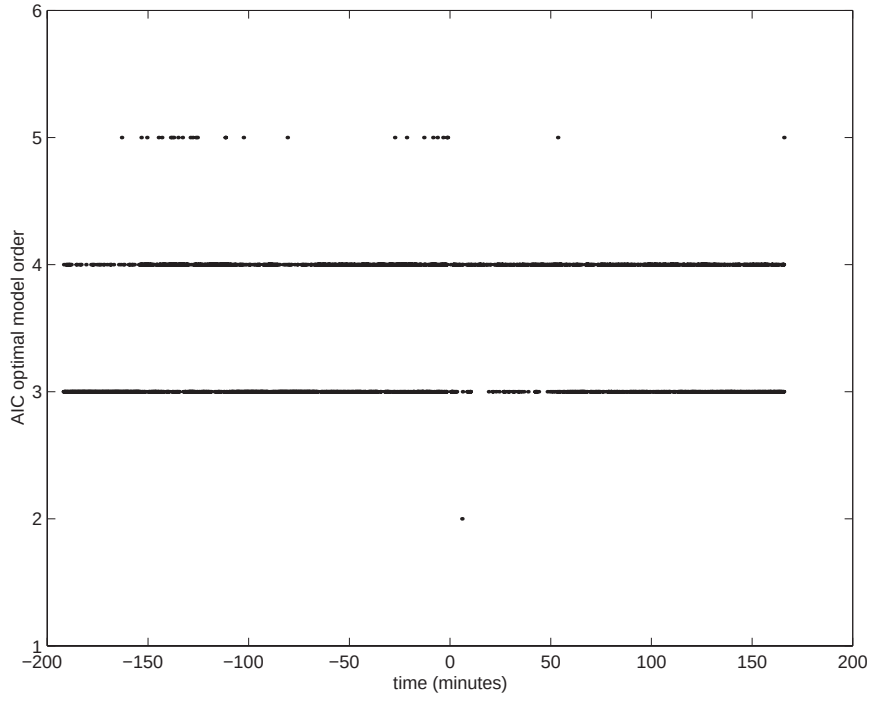

Fig. 2. The plot of values of optimal model order according to the Akaike AIC for 35 channels including depth contacts and temporal lobe subdural contacts in patient 1. Zero on the horizontal scale is at clinical seizure onset. Each point represents the value of the model order for which the AIC has a minimum for a 5-s epoch of data. For 83% of all epochs, the optimal model order was $p = 3$ and for 14% the optimal order was $p = 4$. The values of s for this patient were computed for $p = 3$ and are shown in Fig. 3

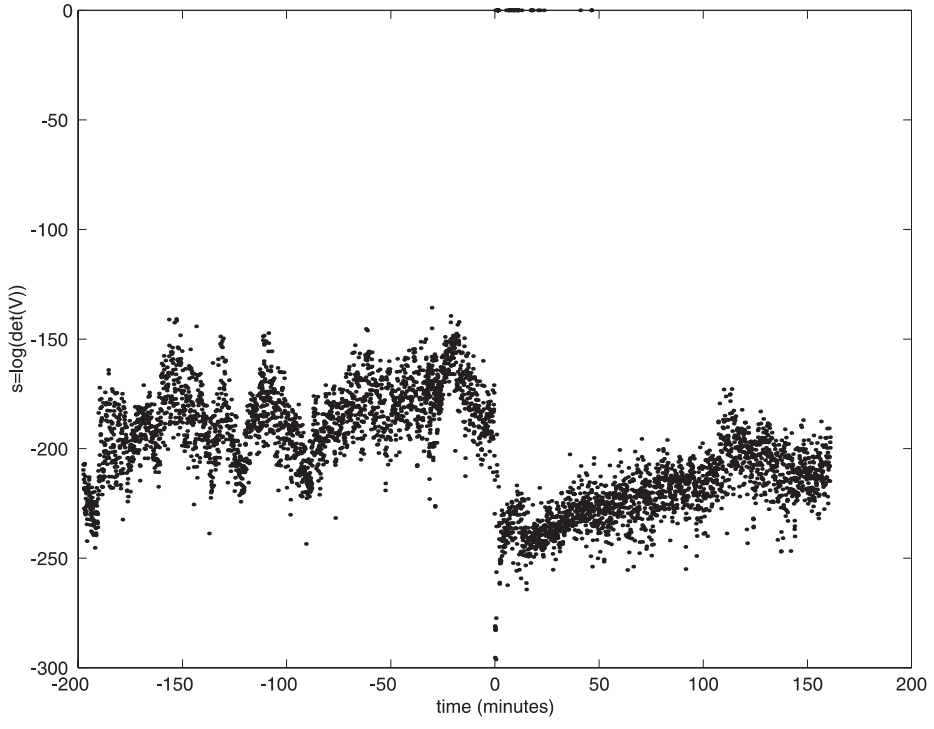

Fig. 3. The plot of $s = \log[\det(\mathbf{V}_e)]$ as a function of time for 35 channels including depth contacts and temporal lobe subdural contacts in patient 1. Zero on the horizontal scale is at clinical seizure onset. Each point represents the value of s computed for a 5-s epoch of recorded ICEEG. The AR model order $p = 3$. Points on the *upper horizontal axis* ($s = 0$) represent epochs for which an autoregressive model was not computed. The value of s remains low for over 2 h after the seizure

for periods of more than 2 h for two patients (Figs. 3–5) and for 30 min (entire available postictal data) in a third patient (Fig. 6).

There were also variations in the values of s before the seizure with several local minima (Fig. 5). These minima correlated with interictal activity, but no subclinical or prolonged electrical seizures were reported or identified by visual video review. In each of the three instances, the actual complex partial seizure lasted less than 116 s; no secondarily generalized seizures were analyzed. In the one seizure with only 30 min of postictal analysis (Fig. 6), postictal slowing lasted less than 10 min. In the other two seizures from the two other patients (Figs. 3–5), postictal slowing lasted less than 20 min.

To test the dependence of the analyses on the number of channels, for one patient we analyzed a smaller groups

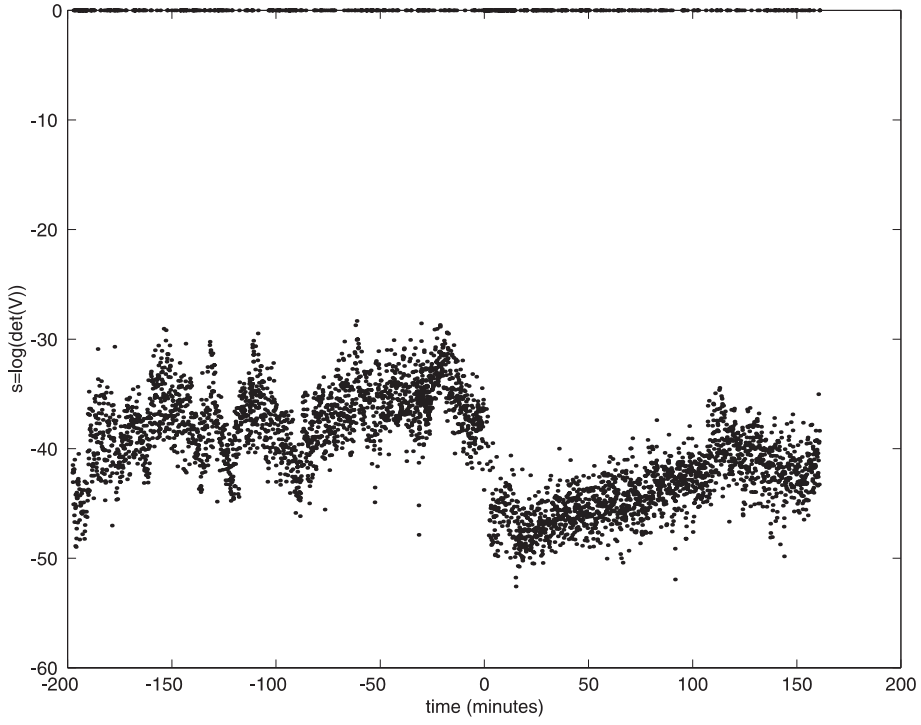

Fig. 4. The plot of $s = \log[\det(\mathbf{V}_e)]$ as a function of time for seven channels including depth contacts and temporal lobe subdural contacts in patient 1. Zero on the horizontal scale is at clinical seizure onset. Each point represents the value of s computed for a 5-s epoch of recorded ICEEG. The AR model order $p = 7$. Points on the upper horizontal axis ($s = 0$) represent epochs for which an autoregressive model was not computed. This plot is very similar to that of Fig. 3

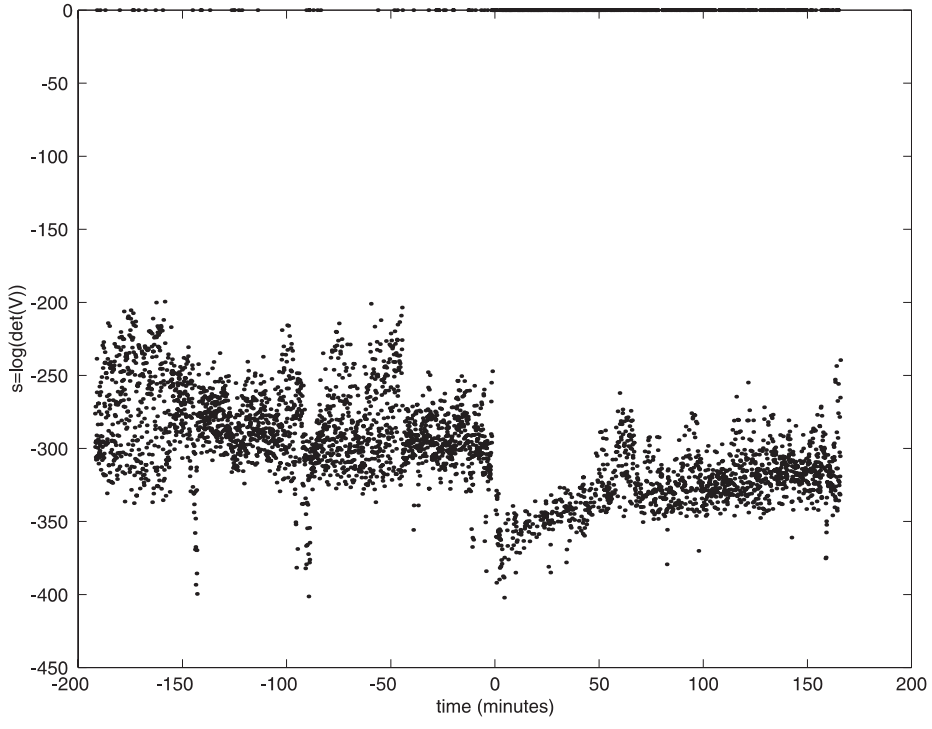

Fig. 5. The plot of $s = \log[\det(\mathbf{V}_e)]$ as a function of time for 31 channels including depth contacts and temporal lobe subdural contacts in patient 2. Zero on the horizontal scale is at clinical seizure onset. Each point represents the value of s computed for a 5-s epoch of recorded ICEEG. The AR model order $p = 4$. Points on the *upper horizontal axis* ($s = 0$) represent epochs for which an autoregressive model was not computed. Again the value of s remains low for some time after the seizure, indicating persistent regional synchrony

of seven channels from the subdural grid, including channels close to the epileptogenic focus (Fig. 4). Patterns of changes in s were similar for all analyses and were not particularly sensitive to selection of the reference. There were noticeably more epochs not suitable for analysis (i.e. $s = 0$) when smaller numbers of channels were included in the analyses. This reflects the fact that more epochs did not have optimal model orders within ± 1 of the preset model. This may indicate a need for a different criterion for choosing a range of acceptable model orders, dependent on the number of channels.

5 Discussion

The quantity s can be interpreted as a measure of order in the system. There is a close relationship between Shannon entropy and residual variance of an auto-

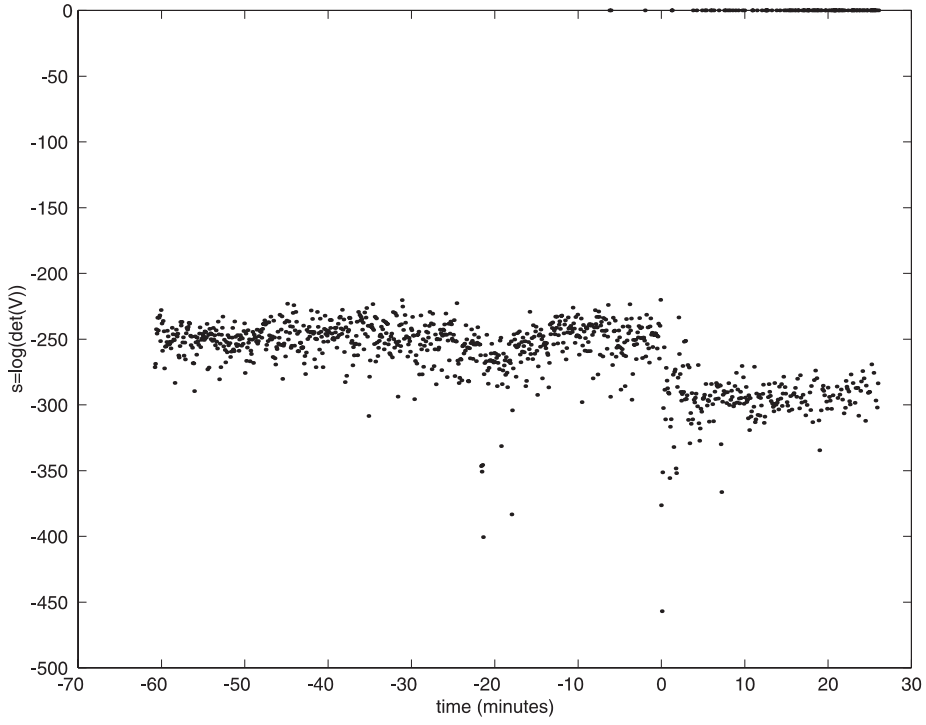

Fig. 6. The plot of $s = \log[\det(\mathbf{V}_e)]$ as a function of time for 45 channels including depth contacts and temporal lobe subdural contacts in patient 3. Zero on the horizontal scale is at clinical seizure onset. Each point represents the value of s computed for a 5-s epoch of recorded ICEEG. The AR model order $p = 2$. Points on the *upper horizontal axis* ($s = 0$) represent epochs for which an autoregressive model was not computed. Regional synchrony as reflected in the value of s persists after the seizure. This record had only 25 min postictal EEG for analysis

regressive process (Serio 1992; Cuomo et al. 1994). The smaller the residual variance, the less information is produced. For example, a periodic system does not produce any new information and is completely predictable. In instances of multichannel processes, high correlation between channels also increases predictability. If channels are highly correlated, one channel can be predicted using other channels, the number of variables necessary to describe dynamics of the system is lower, and the AR model is better fit, resulting in smaller values of s.

Using this approach, we can interpret EEG data in terms of spatial synchrony and the complexity of dynamics of neural networks in the brain. For much of the time, the average level of s is relatively close to zero, reflecting less synchronized and less ordered activity. The minimum of s always occurs shortly after the onset of a seizure. This reflects the high regional synchrony between channels and the very regular, almost periodic, rhythmic activity near the onset of a seizure. This result is in agreement with reports of reduced complexity of brain electrical activity at the beginning of a seizure (Lehnertz and Elger 1995; Pijn et al. 1997), and organized rhythmic activity visible in time-frequency analysis (Franaszczuk et al. 1998). Later, during the seizure, there is an increased number of nonstationary epochs, where s cannot be computed. This, indirectly, may suggest desynchronization and a transitional period to higher complexity. In these patients, 3–20% of the epochs were nonstationary yet even in instances where there are increased nonstationary epochs (e.g. during the seizure), there are sufficient evaluable epochs to yield readily analyzable plots.

The level of synchronization remains higher (s lower) after a seizure for prolonged periods (up to 2 h or more). This may explain in part the phenomena of seizure clustering often seen in patients, if one assumes that increased levels of regional synchronization may increase the likelihood of subsequent seizures. The limited preliminary data do not yet allow for interpretation of the local minima in s observed in periods tens of minutes before seizure onset. Visual inspection of the video-EEG did not identify subclinical or prolonged electrical seizures. Further analysis is needed to correlate this increase in synchrony with occurrences following seizures.

The relatively high and stationary level of s in the interictal EEG remote from seizures reflects much less synchronization. This may reflect either the high complexity of the signal or stochastic system dynamics. These results are also in agreement with reports refuting the presence of low-dimensional chaos in normal EEG (Palus 1996; Theiler and Rapp 1996; Pijn et al. 1997).

The embedding dimension mp is much higher then in typical single channel temporal embedding, usually employed in computations of correlation dimension and Lyapunov exponents. In our analyses the optimal model order p was from 2 for analysis of all 45 channels to 7 for 7 channels close to the epileptic focus. This results in embedding dimensions of 90 and 49, respectively, in the former and latter cases.

There is some controversy about using spatial instead of temporal embedding in analysis of multichannel data. Lachaux (1997), based on simulation of EEG-like signals from well-known dynamical systems placed in a spherical model of the head, suggested that spatial embedding performs better. Prichard and Theiler (1994) found that the evidence for nonlinear structure can be stronger for the multivariate data set than for any of the individual variables. They suggested that the "optimal" embedding will be a combination of some channels and

some time delays. Our method of analysis includes multiple channels and time delays and an embedding dimension that is high enough to account for potentially large number of degrees of freedom in the system.

The measure of synchronization presented here has significant advantages over nonlinear methods of analysis. It is much less computationally complex and can be calculated in real time even for 64 channels simultaneously. Preliminary data suggest that function s can be used for detection of seizure onset. More data is needed to define the suitable threshold level defining seizure onset. A major advantage of this measure is its ability to be interpreted both in the framework of stochastic and deterministic models.

Acknowledgements. We would like to thank our clinical colleagues, Elizabeth Barry, M.D., Kathy Durm, R.N., Howard Eisenberg, M.D., C. Pam Fleming, R.EEGT., and Allan Krumholz, M.D., who assisted in the care of the patients analyzed here.

References

Barry E, Wolf AL, Huhn SL, Bergey GK, Krumholz A (1992) Presurgical evaluation of patients with refractory complex partial seizures using simultaneous subdural grid and depth electrodes. J Epilepsy 5:111–118

Blinowska KJ, Malinowski M (1991) Non-linear and linear forecasting of the EEG time series. Biol Cybern 66:159–165

Casdagli MC, Weigend AS (1993) Exploring the continuum between deterministic and stochastic modeling. In: Weigend AS, Gershenfeld NA (eds) Time series prediction: forecasting the future and understanding the past, vol XV. SFI studies in the sciences of complexity. Addison-Wesley, Reading, Mass, pp 347–366

Casdagli MC, Iasemidis LD, Sackellares JC, Roper SN, Gilmore RL, Savit RS (1996) Characterizing nonlinearity in invasive EEG recordings from temporal lobe epilepsy. Physica D 99:381–399

Cheng B, Tong H (1992) On consistent nonparametric order determination and chaos. J R Stat Soc B 54:427–449

Cuomo V, Serio C, Frisciani F, Ferraro A (1994) Discriminating randomness from chaos with application to a weather time series. Tellus 46A:299–313

Duckrow RB, Spencer SS (1998) Regional coherence and the transfer of ictal activity during seizure onset in the medial temporal lobe. Electroencephalogr Clin Neurophysiol 82:415–422

Elger CE, Lehnertz K (1998) Seizure prediction by nonlinear time series analysis of brain electrical activity. Eur J Neurosci 10:786–789

Franaszczuk PJ, Bergey GK (1998) Application of the directed transfer function method to mesial and lateral onset temporal lobe seizures. Brain Topogr 11:13–21

Franaszczuk PJ, Blinowska KJ, Kowalczyk M (1985) The application of parametric multichannel spectral estimates in the study of electrical brain activity. Biol Cybern 51:239–247

Franaszczuk PJ, Bergey GK, Kamiński MJ (1994) Analysis of mesial temporal seizure onset and propagation using the directed transfer function method. Electroencephalogr Clin Neurophysiol 91:413–427

Franaszczuk PJ, Bergey GK, Durka PJ, Eisenberg HM (1998) Time-frequency analysis using the matching pursuit algorithm applied to seizures originating from mesial temporal lobe. Electroencephalogr Clin Neurophysiol 106:513–521

Gath I, Feuerstein C, Pham DT, Rondouin G (1992) On the tracking of rapid dynamic changes in seizure EEG. IEEE Trans Biomed Eng 39:952–958

Gotman J, Levtova V (1996) Amygdala-hippocampus relationships in temporal lobe seizures: a phase-coherence study. Epilepsy Res 25:51–57

Iasemidis LD, Sackellares JC (1996) Chaos theory and epilepsy. The Neuroscientist 2:118–126

Kamiński M, Blinowska K, Szelenberger W (1997) Topographic analysis of coherence and propagation of EEG activity during sleep and wakefulness. Electroencephalogr Clin Neurophysiol 102:216–227

Kitagawa G, Gersh W (1996) Smoothness priors analysis of time series. Lecture notes in statistics, vol 116. Springer, Berlin Heidelberg New York

Korzeniewska A, Kasicki S, Kamiński M, Blinowska KJ (1997) Information flow between hippocampus and related structures during various types of rat's behavior. J Neurosci Methods 73:49–60

Lachaux J-P, Pezard L, Garnero L, Pelte C, Renault B, Varela FJ, Martinerie J (1997) Spatial extension of brain activity fools the single-channel reconstruction of EEG dynamics. Hum Brain Mapping 5:26–47

Lehnertz K, Elger CE (1995) Spatio-temporal dynamics of the primary epileptogenic area in temporal lobe epilepsy characterized by neuronal complexity loss. Electroencephalogr Clin Neurophysiol 95:108–117

Lehnertz K, Elger CE (1997) Neuronal complexity loss in temporal lobe epilepsy: effects of carbamazepine on the dynamics of the epileptogenic focus. Electroencephalogr Clin Neurophysiol 103:376–380

Marple SL (1987) Digital spectral analysis with applications. Prentice-Hall, Englewood Cliffs NJ

Micheloyannis S, Flitzanis N, Papanikolaou E, Bourkas M, Terzakis D, Arvanitis S, Stam CJ (1998) Usefulness of non-linear EEG analysis. Acta Neurol Scand 97:13–19

Palus M (1996) Nonlinearity in normal human EEG: cycles, temporal asymmetry, nonstationarity and randomness, not chaos. Biol Cybern 75:389–396

Pijn JP, Van Neerven J, Noest A, Lopes da Silva FH (1991) Chaos or noise in EEG signals: dependence on state and brain site. Electroencephalogr Clin Neurophysiol 79:371–381

Pijn JPM, Velis DN, van der Heyden MJ, DeGoede J, Van Veelen CWM, Lopes da Silva FH (1997) Nonlinear dynamics of epileptic seizures on basis of intracranial EEG recordings. Brain Topogr 9:249–270

Prichard D, Theiler J (1994) Generating surrogate for time series with several simultaneously measured variables. Phys Rev Lett 73:951–954

Priestley MB (1981) Spectral analysis and time series. Academic Press, London

Pritchard WS, Duke DW (1992) Measuring chaos in the brain: A tutorial review of nonlinear dynamical EEG analysis. Int J Neurosci 67:31–80

Pritchard WS, Duke DW, Krieble KK (1995) Dimensional analysis of resting human EEG II: Surrogate-data testing indicates nonlinearity but not low dimensional chaos. Psychophysiology 32:486–491

Scott DA, Schiff SJ (1995) Predictability of EEG interictal spikes. Biophys J 69:1748–1757

Serio C (1992) Discriminating low-dimensional chaos from randomness: a parametric time series modelling approach. Nuovo Cimento 107B:681–701

Theiler J (1995) On the evidence for low-dimensional chaos in an epileptic electroencephalogram. Phys Lett A 196:335–341

Theiler J, Rapp PE (1996) Re-examination of the evidence for low-dimensional, nonlinear structure in the human electroencephalogram. Electroencephalogr Clin Neurophysiol 98:213–222

Theiler J, Eubank S, Longtin A, Galdrikian B, Farmer JD (1992) Testing for nonlinearity in time series: the method of surrogate data. Physica D 58:77–94

Wang G, Takigawa M (1992) Directed coherence as a measure of interhemispheric correlation of EEG. Int J Psychophysiol 13:119–128